Dynamic Distribution System Reconfiguration Considering Distributed Renewable Energy Sources and Energy Storage Systems

Sérgio F. Santos ⓘ, Matthew Gough ⓘ, Desta Z. Fitiwi, José Pogeira,
Miadreza Shafie-khah ⓘ, *Senior Member, IEEE*, and João P. S. Catalão ⓘ, *Senior Member, IEEE*

Abstract—Electric power systems are in state of transition as they attempt to evolve to meet new challenges provided by growing environmental concerns, increases in the penetration of distributed renewable energy sources (DRES) as well as the challenges associated with integrating new technologies to enable smart grids. New techniques to improve the electrical power system, including the distribution system, are thus needed. One such technique is dynamic distribution system reconfiguration (DNSR), which involves altering the network topology during operation, providing significant benefits regarding the increased integration of DRES. This paper lays out an improved model which aimed to optimize the system operation in a coordinated way, where DRES, energy storage systems (ESS) and DNSR are considered as well as the uncertainty of these resources. The objective function was modeled to incentivize the uptake of DRES by considering the cost of emissions to incentivize the decarbonization of the power system. Also, the switching costs were modeled to consider not only the switching, but also the cost of degradation of these mechanisms in the system operation. Two systems are used to validate the model, the IEEE 119-bus system, and a real system in São Miguel Island. The results of this paper show that using DNSR, DRES, and ESS can lead to a significant 59% reduction in energy demand through a 24-hour period. In addition, using these technologies results in a healthier, more efficient, and higher quality system. This shows the benefits of using a variety of smart grid technologies in a coordinated manner.

Index Terms—Distribution systems, energy storage systems (ESSs), renewable power generation, stochastic mixed-integer linear programming (SMILP).

NOMENCLATURE

A. Sets/Indices

es/Ω^{es}	Index/set of energy storage.
g/Ω^g	Index/set of generators.
h/Ω^h	Index/set of hours.
l/Ω^l	Index/set of lines.
$n,m/\Omega^n$	Index/set of buses.
s/Ω^s	Index/set of scenarios.
ss/Ω^{ss}	Index/set of energy purchased.
$\varsigma/\Omega^\varsigma$	Index/set of substations.
Ω^1/Ω^0	Set of normally closed/opened lines.
Ω^D	Set of demand buses.

B. Parameters

$d_{n,h}$	Fictitious nodal demand.
$E_{es,n,s,h}^{\min}, E_{es,n,s,h}^{\max}$	Energy storage limits (MWh)/
$\mathrm{ER}_g^{\mathrm{DG}}, \mathrm{ER}_\varsigma^{ss}$	Emission rates of DRES and energy purchased, respectively (tCO_2e/MWh).
$d_l, b_l, S_l^{\max}$	Conductance, susceptance, and flow limit of line l, respectively (Ω^{-1}, Ω^{-1}, MVA).
MP_l, MQ_l	Big-M parameter to the maximum transfer capacity in the system.
n_{DG}	Number of candidate nodes for installation of distributed generation.
OC_g	Cost of unit energy production (€/MWh).
pf_g, pf_{ss}	Power factor of DRES and substation.
$p_{g,n,s,h}^{\mathrm{DG,min}}, p_{g,n,s,h}^{\mathrm{DG,max}}$	Power generation limits (MW).
$p_{es,n,s,h}^{\mathrm{ch,max}}, p_{es,n,s,h}^{\mathrm{dch,,max}}$	Charging/discharging upper limit (MW).
$PD_{s,h}^n, QD_{s,n}^n$	Demand at node n (MW, MVAr).
R_l, X_l	Resistance and reactance of line l (Ω, Ω).
SW_l	Cost of line switching (€/switch).
V_{nom}	Nominal voltage (kV).
$\eta_{es}^{\mathrm{ch}}, \eta_{es}^{\mathrm{dch}}$	Charging/discharging efficiency.
λ^{CO_2}	Cost of emissions (€/tCO_2e).
λ^{es}	Variable cost of storage system (€/MWh).
μ_{es}	Scaling factor (%).
$v_{s,h}^p, v_{s,h}^Q$	Unserved power penalty (€/MWh) (€/MVArh)
ρ_s	Probability of scenarios.

C. Variables

$E_{es,n,s,h}$	Reservoir level of ESS (MWh).
$f_{l,h}$	Fictitious current flows through line l.
$g_{n,h}^{\text{SS}}$	Fictitious current injections at substation nodes.
$I_{es,n,s,h}^{\text{ch}}, I_{es,n,s,h}^{\text{dch}}$	Charging/discharging binary variables.
$P_{g,n,s,h}^{\text{DG}}, Q_{g,n,s,h}^{\text{DG}}$	DG power (MW, MVAr).
$P_{es,n,s,h}^{\text{ch}}, P_{es,n,s,h}^{\text{dch}}$	Charged/discharged power (MW).
$P_{\varsigma,s,h}^{SS}, Q_{\varsigma,s,h}^{SS}$	Imported power from grid (MW, MVAr).
$P_{n,s,h}^{NS}, Q_{n,s,h}^{NS}$	Unserved power (MW, MVAr).
$P_{l,s,h}, Q_{l,s,h}$	Power flow through a line l (MW, MVAr).
$PL_{l,s,h}, QL_{l,s,h}$	Power losses in each feeder (MW, MVAr).
$\chi_{l,h}$	Binary switching variable of line l.
$y_{l,h}^{+} - y_{l,h}^{-}$	Non-negative variables to calculate the absolute difference between sequential switching operations.
$\Delta V_{n,s,h}, \Delta V_{m,s,h}$	Voltage deviation magnitude (kV).
$\theta_{l,s,h}$	Voltage angles between two nodes line l.

D. Functions

$\text{EC}^{\text{DG}}, \text{EC}^{\text{ES}}, \text{EC}^{\text{SS}}$	Expected cost of energy produced by DRES, supplied by ESSs, and imported (€).
$TEmiC$	Expected emission costs of power produced by DRES and imported from the grid (€).
$TENCS$	Expected cost for unserved energy (€).
SWC	Cost of line switching (€).
TEC	Cost of operation (€).

I. INTRODUCTION

A. Motivation

DISTRIBUTION network system reconfiguration (DNSR) has been the topic of discussion for several years. Generally, the research has focused on reducing power losses within a network, network balancing, voltage profile rectification, enhancing network system restoration [1]–[3], network reliability [4], and some combinations of the above goals [5].

The movement towards smart grids has brought a fresh attention to DNSR, mostly around the integration of renewable energy [6], energy storage systems (ESS) [7] or increasing automation of distribution systems. The increasing automation of the distribution system has led to the use of DNSR at both the operational level [1], [8] and planning levels [9], [10]. DSNR has some computational challenges as it is a complex combinatorial problem with many binary variables and constraints. These challenges have been made more difficult by the increase in uncertainty and variability associated with an increase in DRES.

Despite the challenges brought on by distributed renewable energy sources (DRES), these technologies make DNSR important as the distribution system will need to act in a dynamic manner to account for the temporal variability in production and demand. A single reconfiguration is highly unlikely to be the optimal solution over a period. Thus, DNSR is a vital tool in future electricity networks [11] and this is evident from relevant literature [2], [3], [12]–[17].

B. Literature Review

The importance of DNSR to the future energy system mean that some of these challenges associated with its implementation have been explored in the existing literature. For example, a comprehensive multiobjective optimization model to minimize the three-phase unbalance factor and switching times is presented in [18]. A method using graph theory is used to remove infeasible reconfiguration solutions and increase the speed of the developed algorithm. The system is tested on the modified IEEE 34-bus test feeder with two wind power plants and a single solar PV system. This limited number of DRES may not highlight the impact that DRES can have on the network. ESSs were not considered in this model.

A dynamic distribution system reconfiguration model was presented by [19]. In the model, multiple time periods and multiple objective functions were included. Operating costs, power losses and energy not supplied were analyzed. The model was solved using an evolutionary algorithm, more specifically a hybrid between an improved particle swarm optimization and an improved Grey Wolf optimizer. DRES and ESS are not considered, and neither is any form of uncertainty. A 95-bus test system was used withnine generic distributed generation units dispersed through the system.

A procedure for the optimal location and capacity of ESSs was presented by [20]. This procedure included reconfiguration of the distribution grid. The model sought to minimize fluctuations in the voltage profile, reduce the congestion in the lines and reduce investment costs related to the ESS. Uncertainties related to demand and renewable energy generations are considered. The ESS are modeled using the equivalent resistance approach. Uncertainties are handled through a scenario generation approach and then reduced using an approach based on a binary hierarchical cluster tree. PV systems are considered as the DRES. The authors made us of Bender's decomposition to split the problem into a master problem and several subproblems. The master problem was of the mixed-integer quadratically-constrained quadratic programming type and the subproblems were of the second-order cone programming type. Two test networks were considered, a simple six-line system and then the modified 70-bus test system. Results showed a significant improvement in both the quality of supply in the system and to minimize the costs.

A hierarchical structure to manage a distribution system using reconfiguration and in the presence of DRES was presented by [21]. The authors used model predictive control to optimize the system topology and the operational status of the DERs. The model is tested on a 123-bus network. The model considers solar PV generation, generic distributed generation as well as ESSs. The article tried to minimize the cost of energy imported into the system as well as the consumers' discomfort.

A model for the reconfiguration of distribution networks was presented by [22]. This model used a modified particle swarm analysis to determine the optimal network topology

TABLE I
COMPARISON OF PROPOSED MODEL TO EXISTING LITERATURE

Paper	Dynamic reconfiguration	Energy not served	Cost of emissions	Cost of switching	RES Solar PV	RES Wind	Energy Storage System	Uncertainty considered	Type of Optimization	System considered
[18]	X				X	X			Differential Evolution algorithm	IEEE 34-bus system
[19]		X							Evolutionary algorithm	95 bus test system
[20]	X				X		X	X	Mixed-Integer Quadratically-Constrained Quadratic Programming, Second Order Cone Programming type.	6 bus and 70 bus test systems
[21]	X				X		X		Model Predictive Control	IEEE 123 bus test system
[22]	X				X	X		X	Modified PSO	IEE 69 bus test system, 25 bus unbalanced system, 109 bus test system
[23]	X								Semi-definite model	IEEE 34-bus test system, 392 bus test system
[24]	X	X				X		X	Mixed-integer Nonlinear Programming Model	IEEE 34-bus test
[25]	X								Antlion Optimizer	IEEE 33-bus test system.
This Paper	X	X	X	X	X	X	X	X	SMILP	IEE 119 bust system, Real Portuguese Test system

while considering multiple sources of uncertainty such as renewable energy generation and demand. Power losses and voltage stability of the network were considered in the network and the model was tested on both a 69-bus test system, a 25-bus unbalanced system and a real 109 bus system. ESSs were not considered in the model. The two sources of DRES were solar PV and wind energy. The twin objectives of the model were the minimization of the active power losses and the voltage profile deviations. The uncertainties included in the model were modeled using the Monte Carlo technique. The model did not consider costs, either investment, operational or emissions related costs.

A model for the optimal reconfiguration of unbalanced distribution networks considering DRESs was developed by [23]. The model was formulated as a mixed-integer chordal relaxation-based semi-definite model with binary variables. The model was tested on both the IEEE 34-bus test system as well as a 392-bus test system. The model considered capacitor banks, voltage regulators and static var compensators but not battery ESSs. Uncertainty was not considered in the model. Sources of renewable energy generation were not considered. Results show that the model provided significant reductions in operation costs.

Kianmehr *et al.* [24] presented a methodology to optimally coordinate DRES generation from wind farms, ESS and plug in electric vehicles using demand response and network reconfiguration within distribution systems. The objective of the model was to minimize the cost of energy purchased from the DRES and the external grid as well as the fees owed to the consumers for their participation in the demand response program. The model was tested on the IEEE 33-bus test system. The model was formulated as a mixed integer nonlinear programming model. Uncertainty was not incorporated into the model.

A network reconfiguration model considering power losses and quality was developed by [25]. The authors used the antlion optimizer to minimize power losses and improve power quality within the IEEE 33-bus test system. No renewable energy sources or battery ESSs were considered, and neither were forms of uncertainty.

In summary, the problem of DNSR has been examined before in existing literature, however, the inclusion of the emissions costs and the costs of switching in the proposed model sets it apart from the existing literature. In addition, few existing models consider both uncertainty and ESS within the system. The single model that does, namely [20], does not include DRES. These three aspects should be included in a model of DNSR as the renewable sources of energy need to become the dominant forms of energy supply. These sources of energy introduce uncertainty and intermittency which can be mitigates using ESSs. Also, very few papers test their model on real distribution networks to simulate the effects of the DNSR models on existing infrastructure. A summary of the existing literature is given in Table I. The table also shows how the proposed model extends the state of the art through including additional variables in the objective function, the types of DRES considered, the handling of uncertainty as well as running model simulations on a real distribution network.

C. Paper Contributions

The recent literature has given special consideration to the uncertainty and variability associated with renewable energy sources as well as the demand. There is, however, a lack of literature surrounding the use of DNSR in combination with other smart grid technologies. This current work seeks to present

This article has been accepted for inclusion in a future issue of this journal. Content is final as presented, with the exception of pagination.

4

IEEE SYSTEMS JOURNAL

such an analysis. This article then presents the following main contributions.

1) An improved operational model using stochastic mixed-integer linear programming (SMILP), which considers DRES, ESSs, and DNSR and uses an ACOPF formulation
2) An extensive analysis of the implementation of DNSR and smart grid implementing technologies accounting for increased DRES penetration and considering network reliability and stability using two test cases, namely the IEEE 119 bus test system and a real distribution network based on an island power system.
3) Dynamic reconfiguration allowing all the lines within the model to be switchable to provide the optimal solution to the developed SMILP formulation. The costs associated with the switching of the lines is incorporated to account for additional costs imposed on the system through DNSR. Most papers do not consider the costs of switching costs, including the degradation cost of switching.
4) In addition, costs of emissions are also included to better incentivize the uptake of DRES. Existing literature does not include this in the objective function. By including this in the model, the decarbonization of the power system is considered and incentivized.

D. Paper Structure

The rest of the article is structured in the following manner: Section III presents the mathematical description of the proposed model. Section IV contains the information related to the case study as well as the results and discussions from the simulations. Finally, Section V concludes the article.

II. PROBLEM FORMULATION

A. Objective Function

In this article, the model uses a multiobjective approach to minimize the total costs considering the stochastic nature of DRESs (solar and wind) as well as the demand. Therefore, the total costs are minimized considering four cost terms: the cost of switching; the cost of operations; the cost of energy not supplied; and the cost of emissions. The aim of the optimization is to obtain a coordinated model where the benefits of flexibility found using DSR, DR ESS modeling along with an alternating current-optimum power flow (AC OPF) model are verified, for example, in terms of allowing for greater integration of RESs. Therefore, this model presents a linearized AC-OPF-based SMILP model for modeling the electric network system with large-scale integration of DRESs and flexibility options. The resulting model attains the right balance between accuracy and computational complexity. This is also due to the mathematical modeling, where the model was programmed in terms of lines and not of nodes, which reduces the computational requirements, leading to a computationally efficient model.

Therefore, the objective function of the current model sought to minimize the sum of several individual cost terms. The various cost terms are presented in (1) and considered reconfiguration, operation, emissions, and load shed

$$MinTC = SWC + TEC + TENSC + TEmiC. \quad (1)$$

Reconfiguration costs, shown in (2) are incurred when a line changes state, either from open to closed or from closed to open. This cost considers not only the operation but also the cost of switch degradation. This gives the absolute difference between sequential switching operations in time. The absolute difference in (4) is represented by a module, and it can be linearly represented by introducing two non-negative variables: $y_{l,h}^+$ and $y_{l,h}^-$ is therefore expressed by the following equation:

$$SWC = \sum_{l \in \Omega^l} \sum_{h \in \Omega^h} SW_l * (y_{l,h}^+ + y_{l,h}^-) \quad (2)$$

where

$$x_{l,h} - x_{l,h-1} = y_{l,h}^+ - y_{l,h}^-; y_{l,h}^+ \geq 0; y_{l,h}^- \geq 0$$

$$x_{l,0} = 1 \ \forall l \in \Omega^1 \text{ and } x_{l,0} = 0 \ \forall l \in \Omega^0.$$

The sets Ω^1 and Ω^0 refer to the normally closed feeders and tie lines, respectively. The statuses of the feeders and tie lines can change during the optimization period i.e., depending on the optimal topology obtained following the dynamic network reconfiguration.

The costs associated with operation are represented by the total cost of power produced from DG, energy discharged from ESS as well as the emissions associated with importing power from the grid. This is shown in

$$TEC = \sum_{s \in \Omega^s} \rho_s \sum_{h \in \Omega^h} \sum_{g \in \Omega^g} OC_g P_{g,n,s,h}^{\mathrm{DG}}$$

$$+ \sum_{s \in \Omega^s} \rho_s \sum_{h \in \Omega^h} \sum_{es \in \Omega^{es}} \lambda^{es} P_{es,n,s,h}^{\mathrm{dch}}$$

$$+ \sum_{s \in \Omega^s} \rho_s \sum_{h \in \Omega^h} \sum_{\varsigma \in \Omega^\varsigma} \lambda_h^\varsigma P_{\varsigma,n,s,h}^{SS}. \quad (3)$$

Shedding load carries a cost and this cost is accounted for in the model by *TENSC*, in

$$TENSC = \sum_{s \in \Omega^s} \rho_s \sum_{h \in \Omega^h} \left(v_{s,h}^P P_{n,s,h}^{NS} + v_{s,h}^Q Q_{n,s,h}^{NS} \right). \quad (4)$$

Here, $v_{s,h}^P$ and $v_{s,h}^Q$ define penalty parameters for active and reactive power that is not supplied. These two parameters are each set to a sufficiently high value, which roughly quantifies the value of lost load.

The total cost of the emissions is accounted for in (5) which represented the emissions associated with supplying power by DG, discharging energy from ESS or importing from the grid

$$TEmiC = \sum_{s \in \Omega^s} \rho_s \sum_{h \in \Omega^h} \sum_{g \in \Omega^g} \sum_{n \in \Omega^n} \lambda^{CO_2} ER_g^{\mathrm{DG}} P_{g,n,s,h}^{\mathrm{DG}}$$

$$+ \sum_{s \in \Omega^s} \rho_s \sum_{h \in \Omega^h} \sum_{\varsigma \in \Omega^\varsigma} \sum_{n \in \Omega^n} \lambda^{CO_2} ER_\varsigma^{SS} P_{\varsigma,s,h}^{SS}. \quad (5)$$

This article has been accepted for inclusion in a future issue of this journal. Content is final as presented, with the exception of pagination.

SANTOS *et al.*: DYNAMIC DISTRIBUTION SYSTEM RECONFIGURATION CONSIDERING DRESs AND ESSs

5

B. Constraints

The model respects Kirchhoff's law which states that the summation of incoming flows at a specific node should be equal to the sum of the outgoing flows.

This law is respected for both active (6) and reactive power (7) power flows

$$
\sum_{g \in \Omega^g} P^{\mathrm{DG}}_{g,n,s,h} + \sum_{es \in \Omega^{es}} \left(P^{\mathrm{dch}}_{es,n,s,h} - P^{\mathrm{ch}}_{es,n,s,h}\right) + P^{SS}_{\varsigma,s,h}
$$

$$
+ P^{NS}_{n,s,h} + \sum_{in,l \in \Omega^l} P_{l,s,h} - \sum_{out,l \in \Omega^l} P_{l,s,h} = PD^n_{s,h}
$$

$$
+ \sum_{in,l \in \Omega^l} \frac{1}{2} PL_{l,s,h} + \sum_{out,l \in \Omega^l} \frac{1}{2} PL_{l,s,h} \quad \forall \varsigma \in i \qquad (6)
$$

$$
\sum_{g \in \Omega^g} Q^{\mathrm{DG}}_{g,n,s,h} + Q^{SS}_{\varsigma,s,h} + Q^{NS}_{n,s,h} + \sum_{in,l \in \Omega^l} Q_{l,s,h}
$$

$$
- \sum_{out,l \in \Omega^l} Q_{l,s,h} = QD^n_{s,h} + \sum_{in,l \in \Omega^l} \frac{1}{2} QL_{l,s,h}
$$

$$
+ \sum_{out,l \in \Omega^l} \frac{1}{2} QL_{l,s,h} \forall \varsigma \in i. \qquad (7)
$$

Since a line is composed by the interconnection between 2 nodes, the line losses are assigned half to each node. Half of the losses to the node where the power flow starts (in) and half to the node where it ends (out).

Kirchhoff's voltage law, which govern the power flows through each feeder, is also accounted for in the model. Linearized power flow expressions (8) and (9) are used. In these equations, the angle difference between $\theta_{n,s,h} - \theta_{m,s,h}$ is shown by $\theta_{l,s,h}$ with n and m are bus indices which correspond to line l. As a rule-of thumb, the big-M parameter is often set to the maximum transfer capacity in the system

$$
|P_{l,s,h} - (V_{\mathrm{nom}} (\Delta V_{n,s,h} - \Delta V_{m,s,h}) g_l - V^2_{\mathrm{nom}} b_l \theta_{l,s,h}|
$$

$$
\leq MP_l (1 - \chi_{l,h}) \qquad (8)
$$

$$
|Q_{l,s,h} - (-V_{\mathrm{nom}} (\Delta V_{n,s,h} - \Delta V_{m,s,h}) b_l - V^2_{\mathrm{nom}} g_l \theta_{l,s,h}|
$$

$$
\leq MQ_l (1 - \chi_{l,h}). \qquad (9)
$$

The power flowing through a single line has an upper bound which is shown in (10). The power losses associated with active and reactive power are shown in (11) and (12), respectively,

$$
P^2_{l,s,h} + Q^2_{l,s,h} \leq \chi_{l,h} (S^{\max}_l)^2 \qquad (10)
$$

$$
PL_{l,s,h} = R_l \left(P^2_{l,s,h} + Q^2_{l,s,h}\right) \big/ V^2_{\mathrm{nom}} \qquad (11)
$$

$$
QL_{l,s,h} = X_l \left(P^2_{l,s,h} + Q^2_{l,s,h}\right) \big/ V^2_{\mathrm{nom}}. \qquad (12)
$$

Expressions (13)–(18) represent the constraints associated with ESS

$$
0 \leq P^{\mathrm{ch}}_{es,n,s,h} \leq I^{\mathrm{ch}}_{es,n,s,h} P^{\mathrm{ch},\max}_{es,n,s,h} \qquad (13)
$$

$$
0 \leq P^{\mathrm{dch}}_{es,n,s,h} \leq I^{\mathrm{dch}}_{es,n,s,h} P^{\mathrm{ch},\max}_{es,n,s,h} \qquad (14)
$$

$$
I^{\mathrm{ch}}_{es,n,s,h} + I^{\mathrm{dch}}_{es,n,s,h} \leq 1 \qquad (15)
$$

$$
E_{es,n,s,h} = E_{es,n,s,h-1} + \eta^{\mathrm{ch}}_{es} P^{\mathrm{ch}}_{es,n,s,h} - \frac{P^{\mathrm{dch}}_{es,n,s,h}}{\eta^{\mathrm{dch}}_{es}} \qquad (16)
$$

$$
E^{\min}_{es,n,s,h} \leq E_{es,n,s,h} \leq E^{\max}_{es,n,s,h} \qquad (17)
$$

$$
E_{es,n,s,h0} = \mu_{es} E^{\max}_{es,n}; E_{es,n,s,h24} = \mu_{es} E^{\max}_{es,n}. \qquad (18)
$$

The charging and discharging power are bounded by (13) and (14), respectively, and the expression in (15) ensures that charging and discharging cannot occur at the same time.

Equation (16) models the state of charge of the ESS. The storage level of the ESS is bounded by the inequality in (17). The initial and final state of charge is shown in (18). The final state of charge is set to be equal to the initial state of charge.

The power limits of DG for active and reactive power are given in (19) and (20) respectively while (21) places constraints on the ability of the DG to produce or consume reactive power

$$
P^{\mathrm{DG},\min}_{g,n,s,h} \leq P^{\mathrm{DG}}_{g,n,s,h} \leq P^{\mathrm{DG},\max}_{g,n,s,h} \qquad (19)
$$

$$
Q^{\mathrm{DG},\min}_{g,n,s,h} \leq Q^{\mathrm{DG}}_{g,n,s,h} \leq Q^{\mathrm{DG},\max}_{g,n,s,h} \qquad (20)
$$

$$
- \tan\tan\left(\cos^{-1}(pf_g)\right) P^{\mathrm{DG}}_{g,n,s,h} \leq Q^{\mathrm{DG}}_{g,n,s,h}
$$

$$
\leq \tan\left(\cos^{-1}(pf_g)\right) P^{\mathrm{DG}}_{g,n,s,h} \qquad (21)
$$

Limits of the active and reactive power at substations are shown as

$$
P^{SS,\min}_{\varsigma,s,h} \leq P^{SS}_{\varsigma,s,h} \leq P^{SS,\max}_{\varsigma,s,h} \qquad (22)
$$

$$
Q^{SS,\min}_{\varsigma,s,h} \leq Q^{SS}_{\varsigma,s,h} \leq Q^{SS,\max}_{\varsigma,s,h}. \qquad (23)
$$

Bounds are placed on the amount of reactive power withdrawn at a substation are shown as

$$
- \tan\tan\left(\cos^{-1}(pf_{ss})\right) P^{SS}_{\varsigma,s,h} \leq Q^{SS}_{\varsigma,s,h}
$$

$$
\leq \tan\left(\cos^{-1}(pf_{ss})\right) P^{SS}_{\varsigma,s,h}. \qquad (24)
$$

The system under consideration is guaranteed to operate in a radial manner through the introduction of (25)–(31). In addition, islanding caused by DG is prevented by (27)–(31)

$$
\sum_{l \in \Omega^l} \chi_{l,h} = 1 \; \forall m \in \Omega^D; l \in n \qquad (25)
$$

$$
\sum_{in,l \in \Omega^l} \chi_{l,h} - \sum_{out,l \in \Omega^l} \chi_{l,h} \leq 1 \; \forall m \notin \Omega^D; l \in n. \qquad (26)
$$

Equation (25) ensures that nodes with demand at hour h are mandatory to be connected and have a single input flow through line l. The inequality shown in (26) set a maximum of one input flow for the terminal nodes. In this article, DGs are considered, the previous equations are not sufficient to prevent cases where nodes could be supplied by DGs and not connected to the rest of the network. For that reason, the following constraints (27)–(31) are added to avoid isolated generators by modeling a fictitious system with fictitious loads. Such fictitious loads can only be

This article has been accepted for inclusion in a future issue of this journal. Content is final as presented, with the exception of pagination.

6

IEEE SYSTEMS JOURNAL

supplied by fictitious energy through the actual feeders

$$\sum_{\text{in},l\in\Omega^l} f_{l,h} - \sum_{\text{out},l\in\Omega^l} f_{l,h} = g_{n,h}^{SS} - d_{n,h} \ \forall n \in \Omega^\varsigma; l \in n$$
(27)

$$\sum_{\text{in},l\in\Omega^l} f_{l,h} - \sum_{\text{out},l\in\Omega^l} f_{l,h} = -1 \ \forall n \in \Omega^g \ \forall n \in \Omega^D$$
(28)

$$\sum_{\text{in},l\in\Omega^l} f_{l,h} - \sum_{\text{out},l\in\Omega^l} f_{l,h} = 0$$

$$\forall n \notin \Omega^g \ \forall n \notin \Omega^D \forall n \notin \Omega^\varsigma$$
(29)

$$0 \le \sum_{\text{in},l\in\Omega^l} f_{l,h} + \sum_{\text{out},l\in\Omega^l} f_{l,h} \le n_{\text{DG}}; l \in n$$
(30)

$$0 \le g_{n,h}^{SS} \le n_{\text{DG}} \ \forall n \in \Omega^\varsigma; l \in n.$$
(31)

Constraint (27) represents the fictitious nodal current balance equation while constraints (28) and (29) impose limits of fictitious flows through the feeders. Inequality (30) limits the fictitious flow in a line to the number of nodes which could have fictitious generation. The last constraint (31) models the limits for the fictitious currents injected by fictitious substations.

III. CASE STUDY, RESULTS, AND DISCUSSION

A. Systems Description, Assumptions and Data

The proposed model is tested in two different case studies, one being the 119 bus IEEE test system and the other being the system of Lagoa (based on São Miguel Island, Portugal). Details of the systems are presented in [19] and [20], respectively. Simplified representations of the two systems are shown in Figs. 1 and 2. These figures show the locations of DG as well as the ESSs.

Two types of DRES are used in the system, solar PV, and wind. These technologies have an installed capacity of 2 MW and 1 MW, respectively, while the ESS has an installed capacity of 1 MW and charging and discharging efficiencies of 90%.

The 119-bus test system has an active power load of 22.71 MW and a reactive load of 17.04 MVar, while the Lagoa system has an active load of 3.93 MW and a reactive load of 1.62 MVar. An operating period of 24 hours is used in both cases with hourly reconfiguration considered possible for all feeders of the systems.

The system voltage of the 119 bus and the Lagoa system is 12.66 V and 10 kV, respectively, while the maximum allowed voltage deviation is set at ± 5% of the nominal voltage value. The reference node is chosen to be the substation node and the voltage magnitude is set to the nominal voltage and the voltage angle set to 0. A power factor for the substation of 0.95 is used. Electricity prices are allowed us to fluctuate between 42 and 107 €/MWh depending on the demand. The lowest prices occur in the valley periods and the highest prices occur during the peak demand period. Operating costs for the ESS charging and discharging are set at 5 €/MWh.
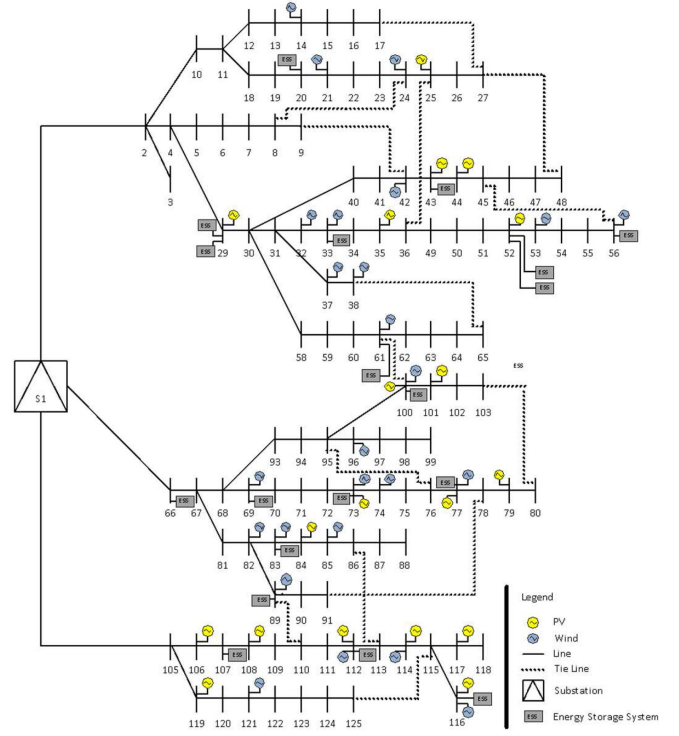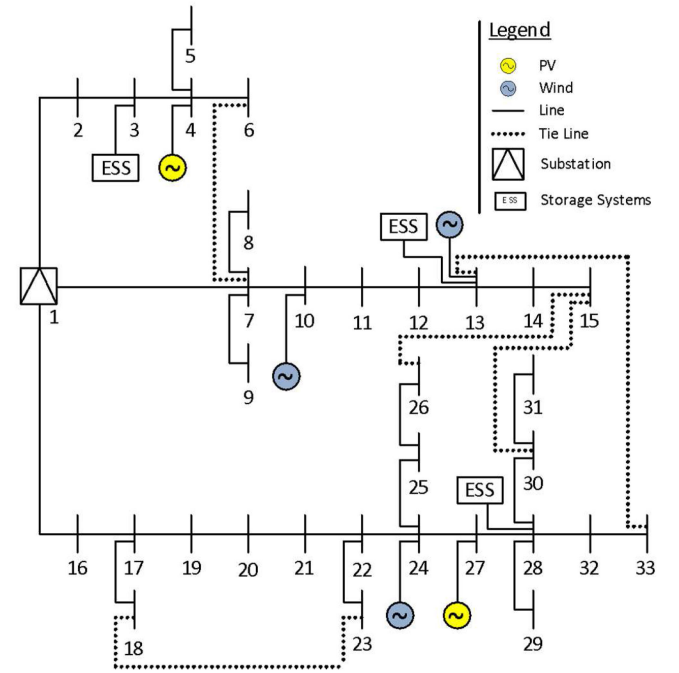

Fig. 1. Adapted 119 bus test system.

Fig. 2. Simplified single line diagram of the considered system [26].

An emission factor of 0.4 tCO2$_e$/MWh is used, and the carbon price is set at 7 €/tCO2$_e$. Electricity generated from the solar PV and wind park costs 40 €/MWh and 20 €/MWh, respectively, and the cost of switching any line is set at 5 € per switch [26]. Uncertainties around demand and the power generation of the two intermittent renewable energy sources (solar and wind)

TABLE II
CONSIDERED CASES

Case	Reconfiguration	DRES	ESSs
A	-	-	-
B	X	-	-
C	X	X	-
D	X	X	X

are considered. These uncertainties are included by considering three scenarios of different hourly profiles as is done in [27].

In this article, scenarios are used for the operational period. A scenario represents a sequence of events of an uncertain parameter. For example, the DRES power output uncertainty is translated by a possible number of story lines. The operation period is the time window where the operation variables are being analyzed. In this article, an operation period of 24 h is defined. In this article, the uncertainty and variability associated to the considered problem are considered through a stochastic process. For a given stochastic parameter, instead of being considered as only a single evolution mode, different possible realizations are considered, each with associated probability. Therefore, the individual scenarios of demand, wind and solar power outputs are combined to form a set of 27 scenarios (i.e., 3*3*3). All these scenarios are expected to be equally probable with ρ_s equal to 1/27.

Four case studies were used in this analysis (cases–D) on both test systems. The details of these cases are given in Table II. Case A is the base case without any reconfiguration, any DG or any ESS. Case B applies reconfiguration to the base case. Various DRES are considered in case C while case D considers both DG and reconfiguration of the system.

B. Results and Discussion

Case A is the base case without any reconfiguration or DRES. Thus, the demand of the system is solely met by importing power through the substation.

The constraints placed on the voltage deviation are relaxed to allow for convergence to a solution as there are not adequate measures to ensure that the voltage magnitude at each of the buses within the predefined limits, especially the voltage magnitudes at the furthest node. This relaxation only happens in case A, for the other cases the voltage deviation restrictions are in place.

Reconfiguration and DRES are often used to solve this issue. Results from case A show energy loses of 30.17 MW for the IEEE test system and 9.47 MW for the Lagoa system. The aggregated hourly active power losses for both systems are shown in Figs. 3 and 4.

The use of reconfiguration carried out in case B helps to reduce the losses within the system. The power losses are reduced from 30.17 to 20.38 MW for the IEEE system when compared to case A and for the Lagoa system, the losses are reduced from 9.47 to 6.07 MW. This equates to a 32.5% and 35.9% reduction in losses for the IEEE and the Lagoa system, respectively. The results for case B are shown as the purple line in Figs. 3 and
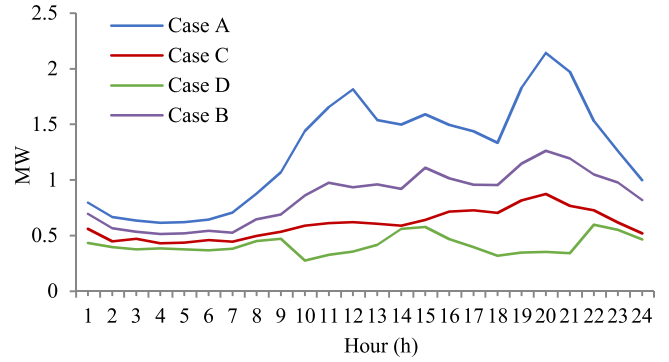

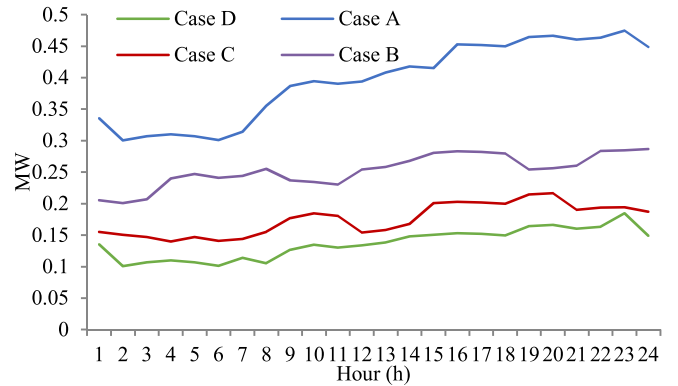Fig. 3. System losses for all cases (119 bus test system).

Fig. 4. System losses for all cases (Lagoa test system).

4. From the figures, case A has higher losses in the peak hours than the shallow and off-peak hours. Reconfiguration (case B) lowers these peak losses and make the power loses more constant across the day. The peak losses in case A are 2.2 and 0.5 MWh and in case B they are 1.3 and 0.3 MWh. This shows that reconfiguration can help to reduce system costs.

The various system reconfigurations for both the IEEE system and the Lagoa system for cases B and D are given in Tables III and IV, respectively. The tables only show the lines that were switched, i.e., the tables do not show those lines that are always connected. The reconfiguration is carried out to meet the demand at all nodes, always and through the various scenarios to provide the least congested path with the lowest *R/X* ratio possible. The reconfiguration is optimally made by the model.

The effects of including DRES are shown in case C along with having dynamic reconfiguration. The DRES have the effect of lowering the demand in the power system relative to case A as the DRES can supply a portion of the required load. This reduction in demand has the effect of reducing the losses in the lines. This can be shown in the decrease in power losses from 52.22% in case B to 29.27% in case C when analyzing the 119 bus IEEE system.

The same happens in the Lagoa system were the expected losses decrease from 30.78% and 55.60% in comparison with cases B and A, respectively.

Including DG into the system significantly affects the energy mix of the two systems relative to both cases A and C as can

TABLE III
NETWORK RECONFIGURATION OUTCOME FOR CASES B AND
D (LAGOA SYSTEM)

Hour	Case B	Case D
	$x_{k,h} = 0$	$x_{k,h} = 0$
1	21; 23; 26; 33; 34	26; 33; 34; 35; 37
2	26; 33; 34; 35; 37	5; 32; 33; 36; 37
3	5; 32; 35; 36; 37	24; 27; 34; 35; 38
4	23; 29; 33; 34; 37	21; 23; 26; 33; 34
5	23; 29; 31; 33; 37	5; 12; 35; 36; 37
6	26; 33; 34; 35; 37	5; 12; 13; 35; 37
7	5; 32; 35; 36; 37	29; 33; 34; 35; 37
8	5; 12; 13; 35; 37	18; 26; 33; 34; 35
9	29; 33; 34; 35; 37	5; 9; 34; 35; 37
10	23; 29; 33; 34; 37	24; 29; 33; 34; 37
11	23; 29; 31; 33; 37	23; 29; 33; 34; 37
12	18; 26; 33; 34; 35	23; 29; 31; 33; 37
13	5; 9; 34; 35; 37	21; 23; 26; 33; 34
14	5; 32; 35; 36; 37	23; 26; 33; 34; 37
15	23; 26; 33; 34; 37	18; 26; 33; 34; 35
16	21; 23; 26; 33; 34	5; 12; 35; 36; 37
17	23; 26; 33; 34; 37	18; 26; 33; 34; 35
18	18; 26; 33; 34; 35	23; 29; 33; 34; 37
19	5; 12; 35; 36; 37	23; 29; 31; 33; 37
20	21; 23; 26; 33; 34	26; 33; 34; 35; 37
21	5; 12; 35; 36; 37	5; 32; 35; 36; 37
22	26; 33; 34; 35; 37	21; 23; 26; 33; 34
23	24; 29; 33; 34; 37	26; 33; 34; 35; 37
24	18; 26; 33; 34; 35	5; 32; 35; 36; 37

Fig. 6.   Case C energy mix for Lagoa test system.

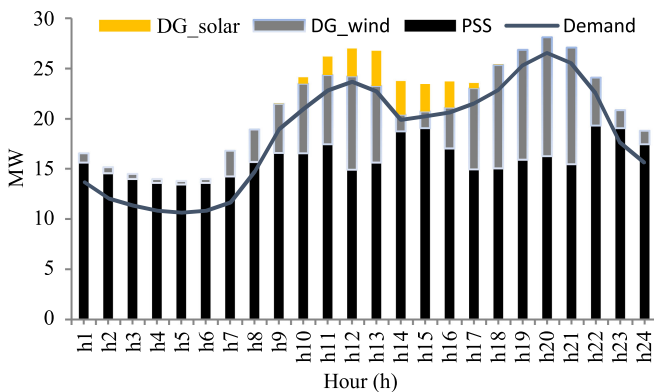Fig. 7.   Case D energy mix for the 119-bus test system.

Fig. 5.   Case C energy mix for the 119-bus test system.

be seen in Figs. 5 and 6. Approximately 40.3% of energy in the 119-bus system and 29.5% in the Lagoa system is provided by DG with wind energy providing the majority of DG power generation as can be expected as wind has the largest proportion of DG within the systems. In addition, some of the DG is not used in the systems. The use of DG has many positive benefits, especially environmentally and economically.

In case D all available technologies (reconfiguration, DRES, and ESSs) are considered. The results of this case, along with the others, are presented in Tables V and VI for the 119-bus system and the Lagoa system, respectively. The energy losses resulting
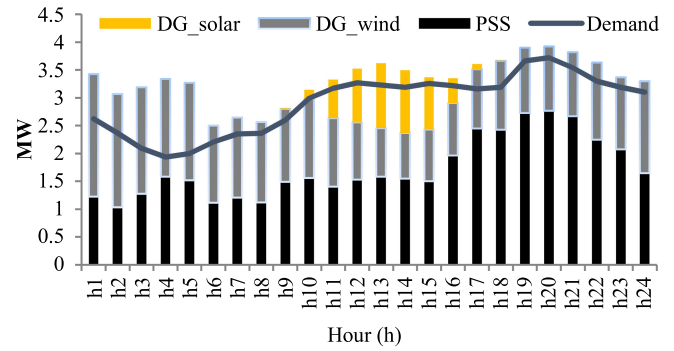
from case D are shown in Figs. 3 and 4 for the respective systems. The reconfigurations done in this case ensure that the topology of the network at any one hour is nearly always different from the topology in another hour.

The lowest overall system cost occurs in case D due to the introduction of DG and ESSs as these technologies contributed significantly to meeting a substantial part of the demand and this also leads to a reduction in the losses.

When DRES are included in the system, they lower the amount of power that needs to be imported from the substation as the DG can partially or fully meet the demand at various nodes. ESSs help to increase these benefits as the ESS can store the energy that otherwise would be lost. ESS can charge during periods of low electricity cost and discharge to help offset higher priced electricity. ESS can also help to reduce the peak demand which increases the health of the system as the number of peak energy demand is lowered.

The active power losses for case D are 10 MW. This represents a decrease of 66.87% 50.95% 30.66%, and relative to cases A, B, and C, respectively, in the 119-bus system. In the case of the Lagoa system, the active power losses are 3.29 MW which is a 65.3%, 45.9%, and 21.83% reduction from cases A, B, and C, respectively. The introduction of the ESS prevents the peak losses from occurring simultaneously with the peak demand.

The energy mic of case D is shown in Figs. 7 and 8 for the 119-bus system and the Lagoa system, respectively. Due to the sizing of the DG and ESS, there is still a portion of demand

TABLE IV
NETWORK RECONFIGURATION OUTCOME FOR CASES B AND D (119 BUS TEST SYSTEM)

	Case B					Case D		
Hour	Open Lines $x_{k,h}=0$	Hour	Open Lines $x_{k,h}=0$		Hour	Open Lines $x_{k,h}=0$	Hour	Open Lines $x_{k,h}=0$
1	26; 39; 61; 74; 85; 118; 120-122; 125; 126; 128; 129; 131; 132	13	23; 34; 61; 74; 82; 85; 117-119; 124-126; 128		1	23; 26; 34; 61; 82; 90; 95; 117; 119; 121; 122; 124; 127; 128; 130	13	23; 26; 34; 53; 61; 90; 95; 119; 121; 124; 127; 128-130; 131
2	23; 26; 34; 53; 61; 82; 85; 90; 95; 119; 121; 124; 127; 128; 131	14	23; 26; 34; 42; 53; 61; 74; 76; 82; 90; 95; 118; 124; 130; 131		2	23; 26; 34; 42; 61; 76; 82; 85; 90; 95; 119; 122; 124; 127; 131	14	23; 34; 61; 74; 82; 85; 118; 119; 121; 122; 124-126; 13
3	23; 26; 34; 53; 61; 74; 82; 85; 119; 121; 124-126; 131	15	23; 26; 34; 39; 53; 61; 74; 118; 121; 125; 128-130; 131		3	23; 26; 34; 61; 74; 76; 82; 85; 90; 95; 119; 121; 122; 124; 131	15	23; 34; 61; 74; 82; 85; 117-119; 124-126; 128
4	26; 34; 39; 53; 61; 85; 118; 120; 121; 125; 126-128;129; 131	16	23; 26; 34; 53; 61; 90; 95; 119; 121; 124; 127; 128-130; 131		4	23; 26; 34; 53; 61; 74; 76; 82; 85; 90; 95; 118; 121; 124; 131	16	23; 34; 39; 53; 61; 85; 118; 119; 121; 125-129; 131
5	23; 26; 34; 61; 82; 85; 90; 95; 119; 121; 122; 124; 126-128; 131	17	23; 26; 34; 39; 53; 61; 90; 95; 119; 121; 127; 130; 131		5	23; 26; 34; 42; 53; 61; 74; 76; 82; 90; 95; 118; 124; 130; 131	17	23; 26; 34; 53; 61; 74; 90; 95; 117; 118; 121; 124; 128-130
6	23; 26; 34; 42; 61; 76; 82; 85; 90; 95; 119; 122; 124; 127; 131	18	23; 26; 34; 53; 61; 74; 76; 82; 85; 90; 95; 118; 121; 124; 131		6	23; 26; 34; 53; 61; 74; 76; 82; 90; 95; 118; 121; 124; 130; 131	18	23; 26; 34; 53; 61; 90; 95; 119; 121; 124; 127-131
7	23; 26; 34; 61; 82; 90; 95; 117; 119; 121; 122; 124; 127; 128; 130	19	23; 34; 39; 53; 61; 85; 118; 119; 121; 125-129; 131		7	23; 26; 34; 42; 61; 74; 76; 90; 95; 119; 122; 124; 129-131	19	26; 34; 39; 53; 61; 85; 118; 120; 121; 125; 126-128; 129; 131
8	23; 26; 34; 42; 61; 74; 76; 90; 95; 119; 122; 124; 129-131	20	23; 34; 61; 74; 82; 85; 118; 119; 121; 122; 124-126; 131		8	23; 26; 34; 53; 61; 82; 85; 90; 95; 119; 121; 124; 127; 128; 131	20	26; 34; 39; 61; 74; 119-122; 125; 126; 128-130; 131
9	23; 26; 34; 53; 61; 74; 76; 82; 90; 95; 118; 121; 124; 130; 131	21	23; 26; 34; 53; 61; 74; 90; 95; 117; 118; 121; 124; 128-130		9	23; 26; 34; 61; 82; 85; 90; 95; 119; 121; 122; 124; 126-128; 131	21	26; 39; 61; 74; 85; 118; 120-122; 125; 126; 128; 129; 131; 132
10	23; 26; 34; 42; 53; 74; 82; 85; 90; 95; 117; 119; 123; 124; 128	22	26; 34; 39; 61; 74; 119-122; 125; 126; 128-130; 131		10	23; 26; 34; 39; 53; 61; 90; 95; 119; 121; 127-130; 131	22	23; 34; 39; 53; 61; 76; 82; 85; 118; 119; 121; 125-127; 131
11	23; 34; 39; 53; 61; 76; 82; 85; 118; 119; 121; 125-127; 131	23	23; 26; 34; 39; 61; 85; 90; 119; 121; 122; 125; 116-129; 131		11	23; 26; 34; 39; 53; 61; 74; 118; 121; 125; 128-130; 131	23	23; 26; 34; 53; 61; 74; 82; 85; 119; 121; 124-126; 131
12	23; 26; 34; 61; 74; 76; 82; 85; 90; 95; 119; 121; 122; 124; 131	24	23; 26; 34; 53; 61; 90; 95; 119; 121; 124; 127-131		12	23; 26; 34; 39; 61; 85; 90; 119; 121; 122; 125; 116-129; 131	24	23; 26; 34; 42; 53; 74; 82; 85; 90; 95; 117; 119; 123; 124; 128

TABLE V
119 BUS TEST SYSTEM: DIFFERENT CASE STUDIES COSTS

	Case A	Case B	Case C	Case D
Total Cost [€]	43217.38	37784.05	33911.80	29912.27
Reconfiguration Cost [€]	0	1050	1120	1010
Energy Cost [€]	40349.82	34452.69	31442.59	27901.72
Emission Cost [€]	2219.56	1743.54	1206.19	1000.55
Cost of power not served [€]	648.00	537.82	143.02	0
Energy Losses [MWh]	30.17	20.38	14.42	10.00

TABLE VI
LAGOA SYSTEM: DIFFERENT CASE STUDIES COSTS

	Case A	Case B	Case C	Case D
Total Cost [€]	5627.86	4947.45	4556.23	3993.00
Reconfiguration Cost [€]	0	620	540	610
Energy Cost [€]	5188.02	4087.42	3841.92	3272.32
Emission Cost [€]	348.36	187.78	139.65	3272.32
Cost of power not served [€]	91.48	52.25	33.66	0
Energy Losses [MWh]	9.47	6.07	4.20	3.29

imported from the grid. Despite this, the energy mix, as well as the reduction in losses and the low voltage deviations, show an increase in the efficiency and quality of the two systems in case D as the various technologies work together in a coordinated manner.

The average voltage deviations for cases A, C, and D are shown in Figs. 9 and 10 for the 119-bus system and the Lagoa system, respectively. Case D shows the smallest voltage deviation as has been discussed previously. Case D can be compared

to case C as it is the same, but Case D also includes ESS. Thus, the difference between the two cases is due to ESS. The ESS improves the voltage profile by approximately 1%.

Tables V and VI highlight the changes in costs across different cases for both systems.

The baseline, case A, has both the highest total cost as well as the highest energy losses. When dynamic reconfiguration is applied, as in the case of Case B, significant cost and energy loss reductions are seen. The costs for Case B decrease by

This article has been accepted for inclusion in a future issue of this journal. Content is final as presented, with the exception of pagination.

10   IEEE SYSTEMS JOURNAL
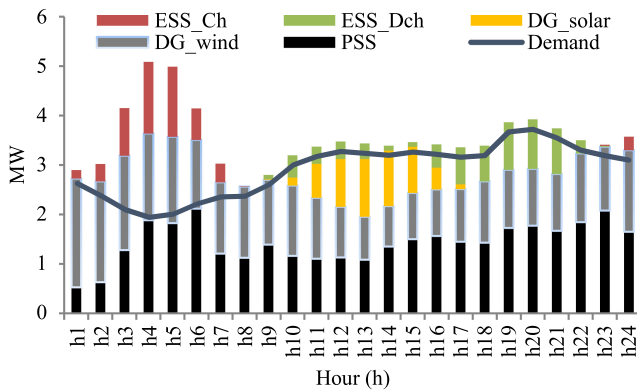

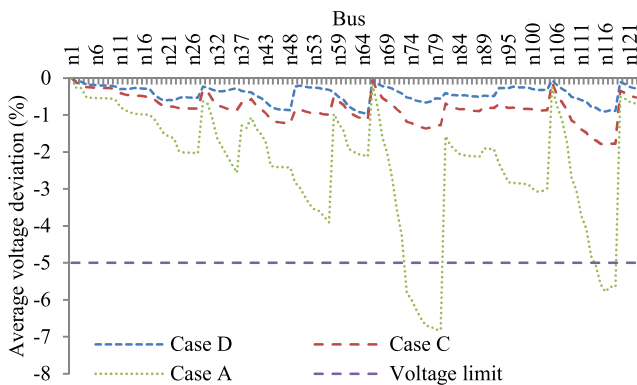
Fig. 8.   Case D energy mix for the Lagoa test system.

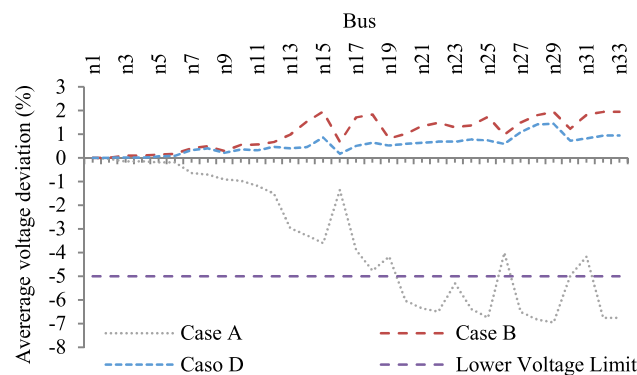Fig. 9.   Average voltage deviation profile of cases A, C, and D in the 119-bus test system.

Fig. 10.   Average voltage deviation profile of Cases A, C, and D in the Lagoa test system.

12.57% for the 119-bus system and 12.1% for the Lagoa system while energy losses decrease by 32% and 36% respectively when compared to case A. Further cost and energy loss reductions are seen when DRES are added to the system as can be seen in case C. Total cost is reduced by 10.25% and 9.73% for the 119-bus and Lagoa system, respectively. There was also a significant reduction in the costs associated with the emissions of both systems.

The trend of cost and energy loss reductions is again shown in case D where ESSs are added to DG and reconfiguration. Relative to case A costs in case D decline by 31% and 29%

for the respective systems. Notably, there is also zero unserved power in case D. This is due to the addition of the ESS which charges during periods of excess generation by the DG. Using the various technologies in case D increase the health and quality of the system while providing significant cost reductions.

IV. CONCLUSION

This article showed the impacts of dynamic reconfiguration on the total costs and energy losses. The benefits of dynamic reconfiguration are further enhanced when distributed generation and ESSs are used in conjunction with dynamic reconfiguration. This article used an improved stochastic MILP to demonstrate these effects on two different test cases, the 119-bus IEEE test system and the Lagoa real case system in São Miguel Island, one of the Azores islands off the coast of mainland Portugal. Each case study used in this article showed the benefits of various technologies in terms of reduced costs, lower energy losses as well as improving the voltage profile of the system. This translates into increases in the decarbonization and efficiency for both the distribution system operator and the customers. Dynamic reconfiguration reduces the voltage deviation within the systems significantly and this effect is amplified when DRES are included in the system. Using ESS provides a small improvement in voltage profile but the major contribution of ESS is to increase the amount of energy produced by the DRES that is stored and used, which would be otherwise lost. This had the effect of reducing the demand, especially at peak times, which led to less energy being imported from the grid, thus less losses in the system and lower costs. The results of this article show that using dynamic reconfiguration, DRES and ESS combined can lead to a major 59% reduction in energy demand through a 24-h period. This shows the benefits of using a variety of technologies, all working together in a coordinated manner. In terms of future work, the impacts of demand response programs can be investigated. In addition, based on these results an investigation into the improvements in system reliability through DNSR and considering DRES should be investigated.

REFERENCES

[1] A. Elmitwally, M. Elsaid, M. Elgamal, and Z. Chen, "A fuzzy-multiagent service restoration scheme for distribution system with distributed generation," *IEEE Trans. Sustain. Energy*, vol. 6, no. 3, pp. 810–821, Jul. 2015, doi: 10.1109/TSTE.2015.2413872.

[2] F. Capitanescu, L. F. Ochoa, H. Margossian, and N. D. Hatziargyriou, "Assessing the potential of network reconfiguration to improve distributed generation hosting capacity in active distribution systems," *IEEE Trans. Power Syst.*, vol. 30, no. 1, pp. 346–356, Jan. 2015, doi: 10.1109/TP-WRS.2014.2320895.

[3] S. Lei, Y. Hou, F. Qiu, and J. Yan, "Identification of critical switches for integrating renewable distributed generation by dynamic network reconfiguration," *IEEE Trans. Sustain. Energy*, vol. 9, no. 1, pp. 420–432, Jan. 2018, doi: 10.1109/TSTE.2017.2738014.

[4] T. Adefarati and R. C. Bansal, "Reliability assessment of distribution system with the integration of renewable distributed generation," *Appl. Energy*, vol. 185, pp. 158–171, Jan. 2017, doi: 10.1016/j.apenergy.2016.10.087.

[5] T. Thakur and T. Jaswanti, "Study and characterization of power distribution network Reconfiguration," in *Proc. Transmiss. Distrib. Conf. Expo.: Latin Amer.*, 2006, pp. 1–6.

[6] Z. Abdmouleh, A. Gastli, L. Ben-Brahim, M. Haouari, and N. A. Al-Emadi, "Review of optimization techniques applied for the integration of distributed generation from renewable energy sources," *Renew. Energy*, vol. 113, pp. 266–280, Dec. 2017, doi: 10.1016/j.renene.2017.05.087.

[7] X. Zhang *et al.*, "Distributed generation with energy storage systems: A case study," *Appl. Energy*, vol. 204, pp. 1251–1263, Oct. 2017, doi: 10.1016/j.apenergy.2017.05.063.

[8] A. K. Singh and S. K. Parida, "A novel hybrid approach to allocate renewable energy sources in distribution system," *Sustain. Energy Technol. Assess.*, vol. 10, pp. 1–11, Jun. 2015, doi: 10.1016/j.seta.2015.01.003.

[9] B. Singh and J. Sharma, "A review on distributed generation planning," *Renew. Sustain. Energy Rev.*, vol. 76, pp. 529–544, Sep. 2017, doi: 10.1016/j.rser.2017.03.034.

[10] A. Keane *et al.*, "State-of-the-art techniques and challenges ahead for distributed generation planning and optimization," *IEEE Trans. Power Syst.*, vol. 28, no. 2, pp. 1493–1502, May 2013, doi: 10.1109/TPWRS.2012.2214406.

[11] A. K. Singh and S. K. Parida, "Need of distributed generation for sustainable development in coming future," in *Proc. IEEE Int. Conf. Power Electron., Drives Energy Syst.*, 2012, pp. 1–6.

[12] L. Bai, T. Jiang, F. Li, H. Chen, and X. Li, "Distributed energy storage planning in soft open point based active distribution networks incorporating network reconfiguration and DG reactive power capability," *Appl. Energy*, vol. 210, no. 2, pp. 1082–1091, Jul. 2017, doi: 10.1016/j.apenergy.2017.07.004.

[13] X. Meng, L. Zhang, P. Cong, W. Tang, X. Zhang, and D. Yang, "Dynamic reconfiguration of distribution network considering scheduling of DG active power outputs," in *Proc. Int. Conf. Power Syst. Technol.*, 2014, pp. 1433–1439.

[14] L. Xu, R. Cheng, Z. He, J. Xiao, and H. Luo, "Dynamic reconfiguration of distribution network containing distributed generation," in *Proc. 9th Int. Symp. Comput. Intell. Des.*, 2016, vol. 1, pp. 3–7.

[15] B. Novoselnik and M. Baotić, "Dynamic reconfiguration of electrical power distribution systems with distributed generation and storage," *IFAC-PapersOnLine*, vol. 48, no. 23, pp. 136–141, 2015.

[16] S. Kennedy and M. M. Marden, "Reliability of islanded microgrids with stochastic generation and prioritized load," in *Proc. IEEE Bucharest PowerTech*, 2009, pp. 1–7.

[17] G. Gutiérrez-Alcaraz, E. Galván, N. González-Cabrera, and M. S. Javadi, "Renewable energy resources short-term scheduling and dynamic network reconfiguration for sustainable energy consumption," *Renew. Sustain. Energy Rev.*, vol. 52, pp. 256–264, Dec. 2015, doi: 10.1016/j.rser.2015.07.105.

[18] C. Peng, L. Xu, X. Gong, H. Sun, and L. Pan, "Molecular evolution based dynamic reconfiguration of distribution networks with DGs considering three-phase balance and switching times," *IEEE Trans. Ind. Informat.*, vol. 15, no. 4, pp. 1866–1876, Apr. 2019, doi: 10.1109/TII.2018.2866301.

[19] A. Azizivahed, E. Naderi, H. Narimani, M. Fathi, and M. R. Narimani, "A new bi-objective approach to energy management in distribution networks with energy storage systems," *IEEE Trans. Sustain. Energy*, vol. 9, no. 1, pp. 56–64, Jan. 2018, doi: 10.1109/TSTE.2017.2714644.

[20] M. Nick, R. Cherkaoui, and M. Paolone, "Optimal planning of distributed energy storage systems in active distribution networks embedding grid reconfiguration," *IEEE Trans. Power Syst.*, vol. 33, no. 2, pp. 1577–1590, Mar. 2018, doi: 10.1109/TPWRS.2017.2734942.

[21] W. Liu and F. Ding, "Hierarchical distribution system adaptive restoration with diverse distributed energy resources," *IEEE Trans. Sustain. Energy*, vol. 12, no. 2, pp. 1347–1359, Apr. 2021, doi: 10.1109/TSTE.2020.3044895.

[22] H. Wu, P. Dong, and M. Liu, "Distribution network reconfiguration for loss reduction and voltage stability with random fuzzy uncertainties of renewable energy generation and load," *IEEE Trans. Ind. Informat.*, vol. 16, no. 9, pp. 5655–5666, Sep. 2020, doi: 10.1109/TII.2018.2871551.

[23] Y. Liu, J. Li, and L. Wu, "Coordinated optimal network reconfiguration and voltage regulator/DER control for unbalanced distribution systems," *IEEE Trans. Smart Grid*, vol. 10, no. 3, pp. 2912–2922, May 2019, doi: 10.1109/TSG.2018.2815010.

[24] E. Kianmehr, S. Nikkhah, V. Vahidinasab, D. Giaouris, and P. C. Taylor, "A resilience-based architecture for joint distributed energy resources allocation and hourly network reconfiguration," *IEEE Trans. Ind. Informat.*, vol. 15, no. 10, pp. 5444–5455, Oct. 2019, doi: 10.1109/TII.2019.2901538.

[25] M. J. H. Moghaddam, A. Kalam, J. Shi, S. A. Nowdeh, F. H. Gandoman, and A. Ahmadi, "A new model for reconfiguration and distributed generation allocation in distribution network considering power quality indices and network losses," *IEEE Syst. J.*, vol. 14, no. 3, pp. 3530–3538, Sep. 2020, doi: 10.1109/JSYST.2019.2963036.

[26] S. F. Santos, D. Z. Fitiwi, M. R. M. Cruz, C. M. P. Cabrita, and J. P. S. Catalão, "Impacts of optimal energy storage deployment and network reconfiguration on renewable integration level in distribution systems," *Appl. Energy*, vol. 185, pp. 44–55, Jan. 2017, doi: 10.1016/j.apenergy.2016.10.053.

[27] E.-E. dos Açores, "Caracterização das redes de transporte e distribuição de energia eléctrica da região autónoma dos açores," 2015, [Online]. Available: https://www.eda.pt/Regulacao/Lists/CaracterizacaodeRedes1/Attachments/26/CARE%202015.pdf